Journal of Solid State Chemistry 182 (2009) 2122–2129

Contents lists available at ScienceDirect

Journal of Solid State Chemistry

journal homepage: www.elsevier.com/locate/jssc

Mesoporous aluminum phosphite

Jamal El Haskouri *, Mónica Pérez-Cabero, Carmen Guillem, Julio Latorre, Aurelio Beltrán, Daniel Beltrán, Pedro Amorós *

Institut de Ciència dels Materials de la Universitat de Valencia (ICMUV), P. O. Box 22085, 46071 Valencia, Spain

ARTICLE INFO

Article history:
Received 17 March 2009
Received in revised form
11 May 2009
Accepted 27 May 2009
Available online 2 June 2009

Keywords:
Mesoporous oxo-phosphorus derivatives
Aluminum phosphates
Template synthesis
Self-assembly

ABSTRACT

High surface area pure mesoporous aluminum-phosphorus oxide-based derivatives have been synthesized through an S^+I^- surfactant-assisted cooperative mechanism by means of a one-pot preparative procedure from aqueous solution and starting from aluminum atrane complexes and phosphoric and/or phosphorous acids. A soft chemical extraction procedure allows opening the pore system of the parent as-prepared materials by exchanging the surfactant without mesostructure collapse. The nature of the pore wall can be modulated from mesoporous aluminum phosphate (ALPO) up to total incorporation of phosphite entities (mesoporous aluminum phosphite), which results in a gradual evolution of the acidic properties of the final materials. While phosphate groups in ALPO act as network building blocks (bridging Al atoms), the phosphite entities become basically attached to the pore surface, what gives practically empty channels. The mesoporous nature of the final materials is confirmed by X-ray diffraction (XRD), transmission electron microscopy (TEM) and N_2 adsorption–desorption isotherms. The materials present regular unimodal pore systems whose order decreases as the phosphite content increases. NMR spectroscopic results confirm the incorporation of oxo-phosphorus entities to the framework of these materials and also provide us useful information concerning the mechanism through which they are formed.

1. Introduction

Investigations at Union Carbide in the early 1980s yielded a new family of crystalline molecular sieves, the aluminophosphates (ALPOs) [1]. With tetra-connected frameworks closely related to those adopted by zeolites [2,3], ALPOs chemistry quickly stirred interest in the search for expanding micropores availability because of potential applications in fields where molecular recognition is needed [2–6]. Due to their significant electronic and structural similarities, it is not surprising that ALPOs chemistry evolved trough similar ways to that of zeolites and tackling also questions as, among others, the expansion of the pore sizes or the functionalization of the material walls [7,8]. In a recent review of Bujoli et al. [9], we can learn about applications of these microporous derivatives in fields like catalysis, environment, biotechnology or medicine.

In practice, the emerging trend of last decades concerning phosphate chemistry is based on (1) the introduction in the reaction medium of a variety of synthetic precursors which might facilitate the formation of open or porous networks having structural and functional analogies with zeolites and (2) the extension of the ALPOs-chemistry through partial or total replacement of aluminum by transition metals and/or phosphate by other tetra or pseudotetrahedral anions [10–12]. In this context, the synthesis of the M41S family of silicas by using surfactants as "supramolecular templates" [13,14] meant the opening of a novel pathway that permitted expanding the typical size of micropores in zeotypes to the mesopore range [15–20]. In that concerning ALPOs, to imitate the chemistry of mesostructured/mesoporous zeolites did not resulted as straightforward as initially might be thought, what has been related to the relative chemical complexity of non-silica materials [21]. This notwithstanding, at the beginnings of the present decade there was already known a diversity of mesostructured and/or mesoporous ALPOs (prepared through surfactant-assisted techniques [22–25]) displaying a variety of topologies, what made possible to outline some tendencies that distinguish them from the related silicas [24]. Although the main result reported in Ref. [24] was the description for the first time of the preparation of mesoporous ALPOs with organically modified surfaces and/or frameworks (a material series denoted as UVM-9 ranging from organic-free AlPOs to pure aluminum phosphonates and diphosphonates), we obtained abundant experimental information concerning, among other aspects, the structural role of condensed aluminum species (Al_{octa}; at difference from silicas) or the self-assembling mechanism through which the UVM-9 materials are formed. The organic functional groups results inserted into the ALPO framework

* Corresponding authors. Fax: +34 96 3543633.
E-mail addresses: haskouri@uv.es (J. El Haskouri).
pedro.amoros@uv.es (P. Amorós).

0022-4596/$ - see front matter © 2009 Elsevier Inc. All rights reserved.
doi:10.1016/j.jssc.2009.05.034

(diphosphonates) or attached to the pore surface (monophosphonates), this last requiring the participation of condensed aluminum species (and departure from the ideal 1:1 stoichiometry) for stabilizing the pore walls.

Without prejudice to the organic substituent, the similarities among monophosphonic acids ($RPO(OH)_2$) and the phosphorous acid ($HPO(OH)_2$) are evident, including not too different pK values. On the basis of the remarkable results obtained in the case of the UVM-9 materials, concerning both the thermal stability and the high surface area of the final materials, we planned to adopt the same preparative technique when considering the possibility of "emptying" the channels of a pure mesoporous monophosphonate by replacing its R functional groups (attached to the pore surface) by covalent bonded H atoms. As in the case of phosphonates, we are also interested in analyzing the structural and chemical effects associated to the progressive introduction of phosphite groups in a pure organic-free ALPO framework. We report here for the first time on the synthesis of both pure mesoporous aluminum phosphite and mesoporous phosphite-modified ALPO by using a simple and well contrasted one-pot surfactant-assisted procedure, which finally yields mesoporous materials displaying high chemical homogeneity as well as good dispersion of the organic groups. Moreover, these materials are the first surfactant-assisted mesoporous phosphite derivatives described in the bibliography.

2. Experimental section

2.1. Synthesis

The method is based on using a cationic surfactant (CTMABr = cetyltrimethylammonimum bromide) as supramolecular template (and, consequently, as porogen after template extraction), and a hydro alcoholic reaction medium (water/triethanolamine, $N(CH_2–CH_2–OH)_3$, hereinafter TEAH3) [26]. In turn, the presence of TEAH3 originates relatively inert alumatrane solutions as source of reactive aluminum species [25–27,31], what has proved its effectiveness for harmonizing (under neutral or slightly basic conditions) the rates of the hydrolytic reactions and the subsequent self-assembling processes among the resulting inorganic polyanions and the surfactant aggregates in related preparations [23–26,28–30].

2.2. Chemicals

All the synthesis reagents are analytically pure, and were used as received from Aldrich [CTMABr, $TEAH_3$, and phosphoric acid] and Fluka [phosphorous acid].

2.3. Preparative procedure

A typical synthesis leading to Sample 3 (aluminum phosphite) is as follows: (1) Preparation of an adequate aluminum precursor from a commercial alkoxide. $Al(OBu^s)_3$ (12.7 mL) was slowly added to liquid $TEAH_3$ (26.2 mL) and heated at 150 °C to give alumatranes. (2) Addition of the structural-directing agent. After cooling of the previous solution to 110 °C, 4.68 g of the CTMABr surfactant were added. (3) Reaction with the phosphorous acid. The resulting solution was cooled to 60 °C and mixed with an aqueous solution of phosphorous acid (6.07 g in 120 mL of water). After a few minutes, a white powder appeared. The resulting (as-prepared) powder was filtered off, washed with water and ethanol and air dried. (4) Surfactant removal. Finally, the surfactant was extracted from the as-synthesized powder using an acetic acid/ethanol solution (ca. 1 g of powder, 16 mL of acetic acid and 130 mL of ethanol) by maintaining the suspension of the as-prepared solid in the alcoholic solution, with stirring, for 24 h at room temperature. The final (mesoporous) material was separated by filtration, washed with ethanol and air dried. A completely equivalent procedure was followed for obtaining solids with phosphate (using phosphoric acid) or mixed phosphate–phosphite entities (using mixtures of phosphoric and phosphorous acids). In all cases, the molar ratio of the reagents was adjusted to 2Al: 3P (H_3PO_4+H_3PO_3): 8$TEAH_3$: 0.52CTMABr: 270H_2O. Table 1 summarizes the main synthesis variables and physical data concerning the materials prepared in this way.

2.4. Physical measurements

All solids were characterized by electron probe microanalysis (EPMA) using a Philips SEM-515 instrument. X-ray powder diffraction (XRD) data were recorded on a Seifert 3000TT θ–θ diffractometer using Cu$K\alpha$ radiation. Patterns were collected in steps of 0.02° (2θ) over the angular range 1°–10° (2θ) for 25 s/step. In order to detect the presence of some crystalline bulk phase, additional patterns were recorded with a larger scanning step (0.05° (2θ)) over the angular range 10°–60° (2θ) for 10 s/step. An transmission electron microscopy (TEM) study was carried out with a JEOL JEM-1010 instrument operating at 100KV and equipped with a CCD camera. Surface area, pore size and volume values were calculated from nitrogen adsorption–desorption isotherms (−196 °C) recorded on a Micromeritics ASAP-2010 automated analyzer. Calcined samples were degassed for 12 h at 110 °C and 10^{-6} Torr prior to analysis. Thermogravimetric analysis (TGA) was performed using a SETARAM SETSYS 16/18 analyzer working under a flowing oxygen atmosphere at 25 ml/min. Prior to the analysis, all samples were stored in a controlled atmosphere with a 30% humidity in order to obtain adequate comparative data. All samples were heated from room temperature until 1000 °C with a heating rate of 5 °C/min. ^{31}P and ^{27}Al NMR spectra of samples stored under controlled humidity conditions were recorded on a Varian Unity 300 spectrometer. Determination of surface acidity was carried out by thermoprogrammed desorption (TPD) of ammonia in a Micromeritics TPD-TPR 2900 apparatus. Samples (about 250 mg) were placed in a quartz reactor connected to the system and pretreated in an helium stream (50 ml/min) up to 300 °C for 1 h, at a rate of 10 °C/min. Samples were then cooled down at 100 °C, saturated with ammonia (10% in helium) for 1 h and then flushed with helium for 1 h more to fully remove physisorbed ammonia. TPD experiments were run under helium flow (50 ml/min) and the amount of desorbed ammonia was measured by a TCD detector. The TPD-NH_3 desorption curve was recorded at a rate of 5 °C/min from room temperature to 300 °C.

3. Results and discussions

3.1. Synthesis

As mentioned above, the method reported here to prepare new mesoporous aluminum phosphite solids was previously optimized (and discussed in detail) for obtaining mesoporous aluminum phosphonates and diphosphonates (denoted as UVM-9 materials) [23,24]. Assuming similar mechanistic principles, suffice is to say now that we have followed here the same protocol for determining the optimized conditions to have polyanionic entities capable of generating the adequate parent mesostructures by interacting (S^+I^- mechanism) with the $CTMA^+$ entities. In light

Table 1
Selected synthetic and physical data for Al-phosphite/phosphate mesoporous materials.

Sample	Phosphorous acid solution (%)	Phosphorous acid solid (%)[a]	Al/P[b]	d_{100} (XRD) (nm)	a_0 (nm)[c]	S_{BET} (m^2/g)	BJH pore[d] (nm)	Pore vol. (cm^3/g)	Pore wall[e] (nm)
1	–	–	1.10(2)	4.95	5.71	633.2	3.23	0.70	2.48
2	50	49	1.26(2)	5.01	5.78	432.5	2.71	0.32	3.07
3	100	100	1.30(2)	5.35	6.17	510.2	2.53	0.36	3.64

[a] Values referred to *P*(phosphite)/*P*(total) molar ratio.
[b] Values averaged from EPMA of ca. 50 particles.
[c] Cell parameters calculated assuming a MCM-41 like hexagonal cell ($a_0 = 2 * d_{100}/3^{1/2}$).
[d] Pore diameters calculated by using the BJH model on the adsorption branch of the isotherms.
[e] Pore wall defined as $a_0 - \phi_{BJH}$.

of the well known significant deviations from the ideal 1:1 stoichiometry [23,24,29–36] towards defective phosphorus compositions in phosphonates and other mesoporous ALPOs, we tried to achieve a working Al:P ratio as low as possible looking for favor the Al–P–Al alternation in the inorganic walls. After checking a variety of Al: *x*P (H_3PO_4+H_3PO_3): 4TEAH3: 0.26CTMABr: 135H_2O starting "compositions", the Al: *x*P (H_3PO_4+H_3PO_3) molar ratio of the reagents was fixed to the final 2Al:3P value, which is the same used in the UVM-9 syntheses. This is not surprising considering that the only difference between the methylphosphonic acid and the phosphorous acid is the change of a terminal CH_3 group by an H atom ($pK_2 = 7.54$ and 6.7, respectively [37,38]). The apparent pH value (ca. 8 for $x = 1.5$) remains practically unaltered for each *x* value (irrespective of the H_3PO_4/ H_3PO_3 relative amounts) because of the buffering effect provided by the $TEAH_3$–H_3PO_4–H_3PO_3 system ($pK_2 = 7.2$, 6.7, and 7.8 for phosphoric acid, phosphorous acid and triethanolamine, respectively) [37,38]. Control of pH (together with a defective initial proportion of Al) seems to be critical in avoiding undesired aluminum excesses in the final materials.

The dominant oxophosphate species under the reaction conditions in rich aqueous media are $HPO_4^{2-} \gg PO_4^{3-}$ and HPO_3^{2-} [39]. With regard to the aluminum species, in the absence of phosphorus oxoanions, the tetrahedral $Al(OH)_4^-$ ions are majority at pH > 5 (as resulting from the $Al(H_2O)_6^{3+}$ hydrolysis), and evolve towards hydrated $Al(OH)_3$ (involving μ-(hydroxo)aluminum chains; Al_{octa}) at increasing pH [39]. The presence of oxophosphate species must drive the system towards the formation of aluminophosphate and/or aluminophosphite complex anions involving, very likely, the presence of terminal and/or aluminum-bridging hydroxyl groups. At some point of these hydrolytic and condensation processes, we will have in solution polyanions adequate for matching with $CTMA^+$ and generate the corresponding mesostructure.

In order to avoid mesostructure collapse during surfactant removal [24,40–42], we extracted the organic template by using acetic acid/ethanol solutions. According to EPMA results, this extraction procedure does not alter the aluminum and phosphorus contents (the corresponding as-prepared and mesoporous extracted solids have identical Al:P molar ratios).

3.2. Characterization

We have used EPMA to check the chemical homogeneity of the resulting solids. Summarized in Table 1 are the corresponding Al:P molar ratio values. EPMA shows that all samples are chemically homogeneous at the micrometric level (spot area ca. 1 μm) with a constant and well-defined composition. At difference from the aluminum phosphate (whose Al:P molar ratio is close to the 1:1 value typical of stoichiometric ALPOs), the aluminum phosphite

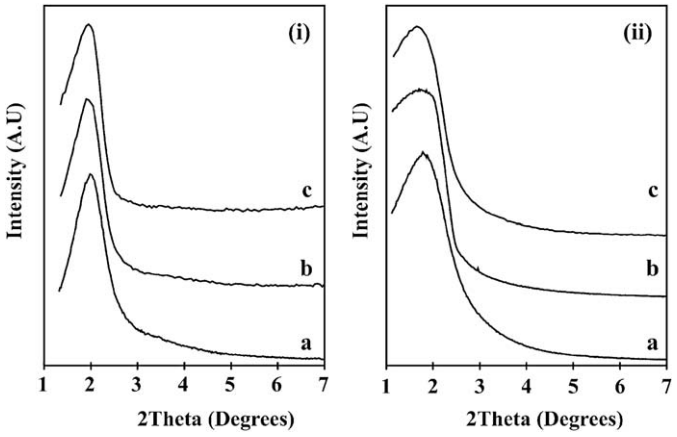

Fig. 1. Low-angle XRD patterns of: (i) as-prepared and (ii) extracted Al-phosphite materials (pure ALPO and Al-phosphate/phosphite): (a) Sample 1, (b) Sample 2, and (c) Sample 3.

solids are phosphorus defective, with Al:P molar ratios close to 1.3, a result that nicely fits with previous observations on monophosphonate materials (Al:P ca. 1.25) [23,24]. On the other hand, the high-angle XRD patterns do not show peaks associated to segregated aluminum-containing bulk phases. This fact, together with the impossibility to condense oxo phosphorus groups among them (originating P–O–P bonds) in aqueous media, allows us to propose that all the synthesized mesoporous materials display regular distributions of the Al and P atoms along the pore walls at micrometric level. In any case, the lack of segregated bulk phases in these phosphorus defective solids would be consistent with the presence of aluminum rich domains (very likely six-coordinated Al) at the nanoscale range. The high chemical homogeneity and dispersion of Al and P atoms indicates that the control of the reactivity that we achieved when using alumatranes as an aluminum source in water–phosphoric media [22] is maintained when phosphoric acid is partially or totally replaced by phosphorous acids.

Shown in Fig. 1 is the evolution of the low-angle XRD patterns with the phosphite content in both the as-prepared and extracted mesoporous solids. In all cases, the XRD patterns include only one strong diffraction peak, which is typical of mesostructured/mesoporous materials prepared through surfactant-assisted procedures. This peak is usually associated with the (100) reflection when a MCM-41-like lattice is assumed. In the case of the as-prepared derivatives (Fig. 1(i)), the absence of any additional diffraction peak in the patterns of the phosphite-containing solids (Fig. 1(i)b, c) is characteristic of disordered hexagonal (H_d) or wormhole-like pore systems. Also, the evolution of the (100) *fwhm* indicates an increasing disorder with the

phosphite content. When comparing the mesoporous materials (Fig. 1(ii)) with their corresponding as-prepared parents (Fig. 1(i)), we can observe that the surfactant evolution results in a significant broadening of the intense (100) peak together with a shift in its position towards lower 2θ values, what agrees with previous results on related mesoporous ALPOs [43,44]. It can be then concluded that surfactant removal implies a significant loss of order in the pore system, in spite of the soft chemical extraction procedure we have used. On the other hand, the d_{100} reticular distance (and consequently the a_0 cell parameter) increases with the phosphite content (see Table 1), this occurring for both the as-prepared and extracted series. This fact is very likely related to the net-connectivity lowering that accompanies the progressive incorporation of terminal HPO_3^{2-} units, as occurs for monophosphonate UVM-9 materials [23,24]. When pseudo-tetrahedral terminal groups (as H-PO_3^{2-} or R-PO_3^{2-}) are dominant (what implies also phosphorus defective compositions), the wall surface may be thought of as mainly defined by an alternating network of aluminum centers and phosphonate terminal units. In contrast, the necessarily more rich aluminum wall cores must include alumina-like (six-coordinated) centers, this favoring a certain increase of the a_0 lattice parameter. It also must be noted that the d_{100} (100) signal appears clearly defined (with a marked maximum) even for the mesoporous solid with the maximum phosphite content (Sample 3, Fig. 1(ii)c), what differs from that observed in the case of the related monophosphonate derivatives (where this d_{100} signal appears as a shoulder) [23,24]. This nice difference suggests that the replacement of R radicals by small H atoms in terminal groups (T-PO_3^{2-}) results in mesoporous materials displaying a comparatively higher order degree. This fact should be probably related to a relaxation of steric hindrances (spatial requirements of $\equiv$P–H vs. $\equiv$P–R) in the course of the self assembling processes with surfactant micelles, which also should be consistent with the observed decrease in the d_{100} and a_0 values of the Samples 2 and 3 with regard to the corresponding UVM-9 monophosphonates [23,24]. In other words, the small terminal P–H entities must lead to a low "surface roughness" without significant constrains affecting the S^+I^- interactions among the inorganic portions and the surfactant micelles.

In any case, the experimentally observed smooth variation of the broadness and position of the (100) peak in the XRD patterns of the mesoporous materials, allows recognize in them a certain character of "solid solution". All the evidence indicates that we are dealing with materials having a reasonably good statistical distribution of phosphate and/or phosphite moieties in the walls. TEM micrographs (Fig. 2) fully correlate to XRD data. In all cases, we can observe a dominant (single-type) particle morphology (with highly disordered hexagonal or wormhole-like pore system arrays), what supports the monophasic nature of the solids and allows discarding phase-segregation processes.

Mesoporosity of the final phosphate and/or phosphite materials is further illustrated by the N_2 adsorption–desorption isotherms (Fig. 3). In all cases, the curves show one well-defined step at intermediate partial pressures ($0.3 < P/P_0 < 0.8$) characteristic of Type IV isotherms (as defined by the IUPAC). This adsorption should be due to the capillary condensation of N_2 inside the pores, and is related to a pore diameter in the mesopore range. However, there are two relevant features in the isotherms (b, c) of the phosphite containing materials: (1) the absence of any hysteresis loop (which is present in the case of both the phosphate (a) and the UVM-9 phosphonate isotherms [23,24]) and (2) the sharpness of the adsorption step, what indicates the uniformity of the mesopore sizes (as supported by the absence of hysteresis loop phenomena). On the other hand, the pore sizes (estimated by using the absorption branch of the isotherms and applying the BJH model) in both phosphite materials are similar

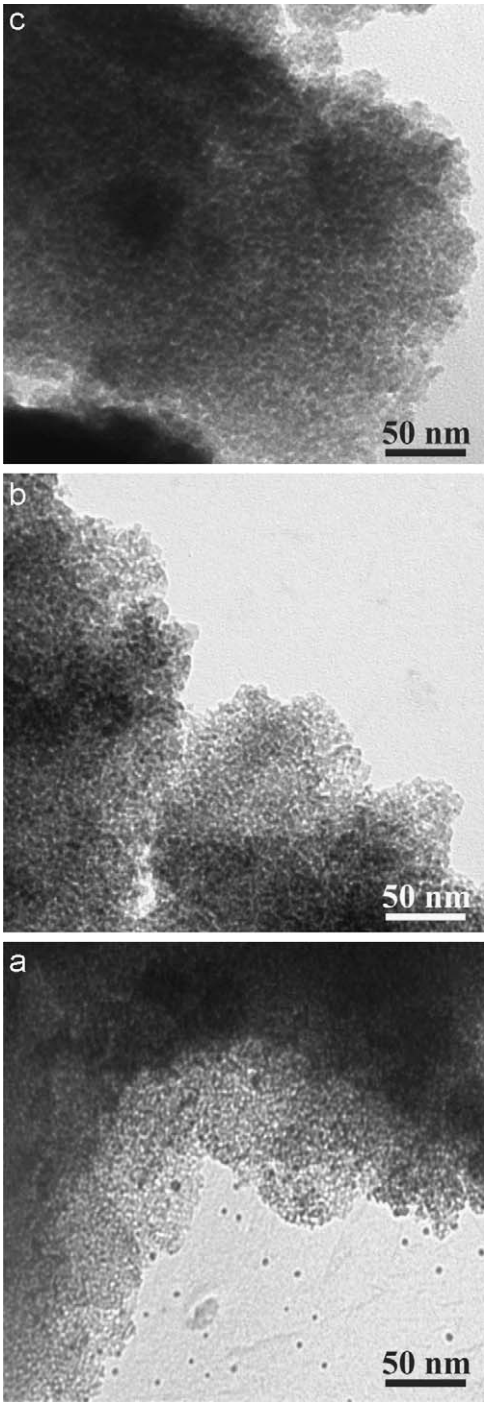

Fig. 2. Selected TEM micrographs: (a) Sample 1, (b) Sample 2, and (c) Sample 3.

(2.7–2.5 nm). In practice, the pore size dispersion in their compositionally homologous methylphosphonates is significantly higher (2.9–3.3 nm) [23,24]. It seems reasonable to relate both the dispersion and difference in pore sizes to the presence of CH_3 groups (instead H atoms) attached to the pore surface in the case of the aluminum phosphonate materials. The relatively small pore sizes seem to be in the origin of the comparatively small BET surface areas and pore volumes of the phosphites with regard to those of the analogous phosphate (Table 1) and phosphonates [23,24]. Notwithstanding, the resulting surface areas ($>500\,m^2/g$) and pore volumes (ca. $0.35\,cm^3/g$) in the phosphites are typical of mesoporous materials with good pore homogeneity, and even can

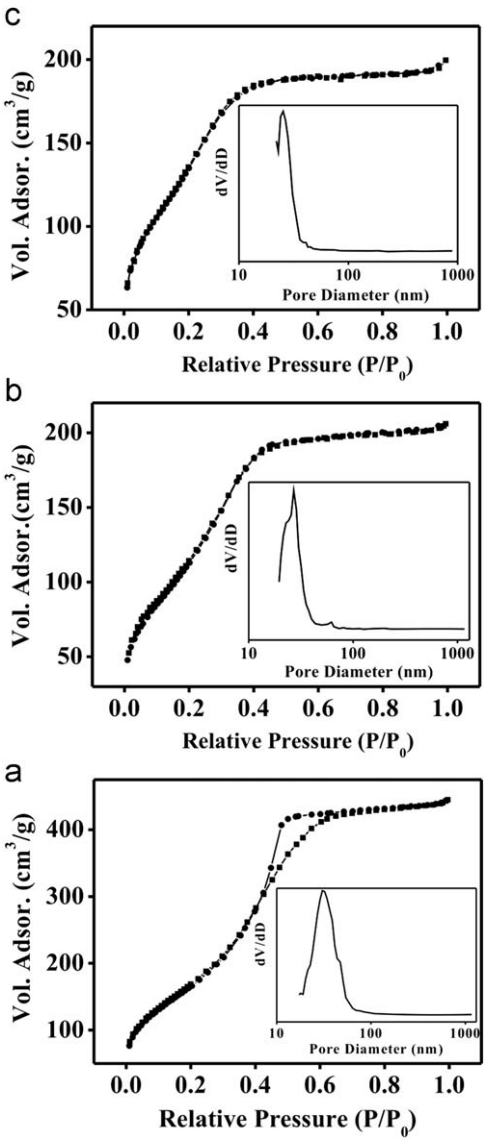

Fig. 3. N_2 adsorption–desorption isotherms for ALPO and Al-phosphate/phosphite derivatives: (a) Sample 1, (b) Sample 2, and (c) Sample 3. The insets show the BJH pore size distributions from the adsorption branch of the isotherms.

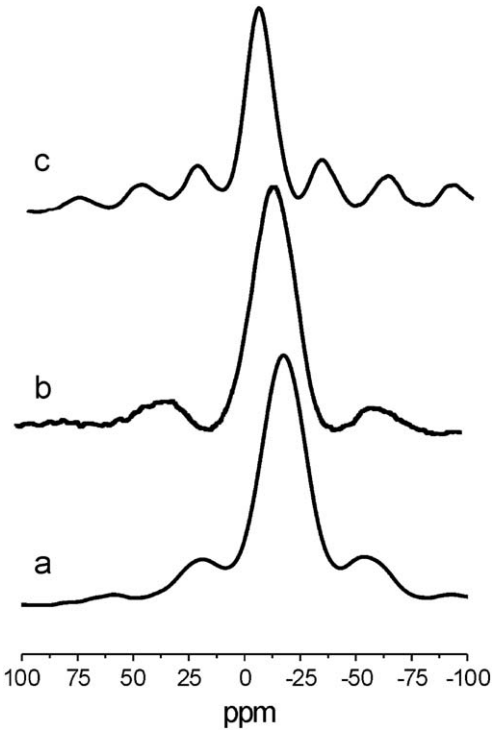

Fig. 4. ^{31}P MAS NMR spectra of dehydrated samples (ALPO and Al-phosphate/phosphite derivatives): (a) Sample 1, (b) Sample 2, and (c) Sample 3.

be considered unusual for non-silica based materials. The thickness of the pore walls (measured as $W_t = a_0 - \phi_{BJH}$) increases with the phosphite content (3.07–3.64 nm). A similar evolution was previously observed for aluminum phosphonates, and it should be probably related to the increase in the proportion of six-coordinated aluminum sites (see below). In short, the progressive incorporation of phosphite groups in the ALPO mesostructure finally leads to mesoporous materials with small and uniform pore sizes, but no pore blocking or necking occurs.

Mesoporous ALPOs are usually classified as high hydrophilic materials due to factors such as: (a) the presence of relatively high concentrations of defect Al–OH and P–OH sites, (b) the capability of four-coordinated Al centers at the surface to increase their coordination number (to give five- or six-coordinated Al sites) by incorporation of OH^- or H_2O groups as ligands, and (c) the electronegativity difference between the Al (1.5) and P (2.1) atoms. In our case, the replacement of terminal P–OH by P–H groups (increasing the proportion of Al–OH moieties) does not affect the surface ability to establish hydrogen bonding interactions with water molecules. In fact, the Samples 1 (phosphate) and 3 (phosphite) display TGA curves with a first weight loss (up to 200 °C) associated to the elimination of a ca. 19 %wt of water. As expected, the hydrophilic nature of these materials is higher than in the case of the related UVM-9 phosphonates. In this last case, the incorporation of P–CH_3 moieties clearly favors lower water contents (ca. 13%). Then, it might be possible to modulate in a certain range the hydrophilic nature of the materials by obtaining intermediate compositions involving both phosphite and phosphonate groups.

^{31}P MAS NMR spectra (Fig. 4) confirm the incorporation of phosphate and/or phosphite groups in the final mesoporous materials and, moreover, clearly reflect the evolution of the phosphorus environment with the phosphite content. Thus, the spectrum (Fig. 4a) of the Sample 1 (ALPO) shows one single downfield shifted signal centered at −25 ppm, which can be attributed to tetrahedral phosphates connected to aluminum centers [43,45]. The spectrum (Fig. 4c) of the pure aluminum phosphite material (Sample 3) also shows only one environment for the P atoms (both before and after surfactant removal), but the corresponding signal appears now centered at −6.1 ppm. Finally, in the case of the Sample 2, the spectrum (Fig. 4b) displays a broad signal centered at an intermediate $\delta \approx -15$ ppm, which can be accordingly attributed at two different phosphorus environments (phosphate and phosphite). Deconvolution of this spectrum is consistent with the presence of 51% of phosphate and 49% of phosphite (see Table 2). These results indicate that there is no preferential incorporation of HPO_4^{2-} vs. HPO_3^{2-} groups into the mesostructure. In fact, the final phosphate/phosphite content in the materials is practically coincident with the proportion of these species in the mother liquor. Moreover, the NMR data confirm that the soft chemical treatment used to extract the surfactant allows us to maintain the chemical integrity of the phosphite groups in the final mesoporous solids. Otherwise, all the prepared solids originate ^{27}Al MAS NMR spectra including two resonance signals of different intensities appearing at δ values of approximately 0

Table 2
NMR data of anhydrous Al-phosphite/phosphate mesoporous materials.

^{31}P NMR					^{27}Al NMR			
Sample	δ ppm phosphate	% phosphate	δ ppm phosphite	% phosphite	δ ppm T_d	% T_d	δ ppm O_h	% O_h
1	−25	100	–	–	44.8	63	−8.9	37
2	−21.5	51	−15.5	49	51	29	−1.5	71
3	–	–	−6.1	100	53.6	16	−1.6	84

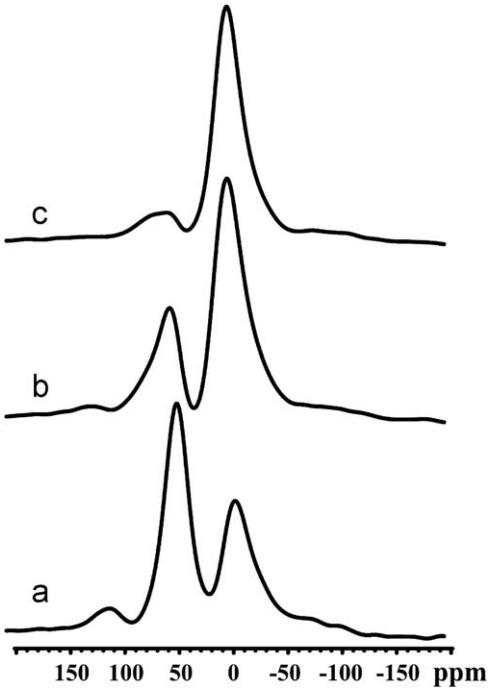

Fig. 5. ^{27}Al MASNMR spectra of dehydrated Al phosphite materials (ALPO and Al-phosphate/phosphite derivatives): (a) Sample 1, (b) Sample 2, and (c) Sample 3.

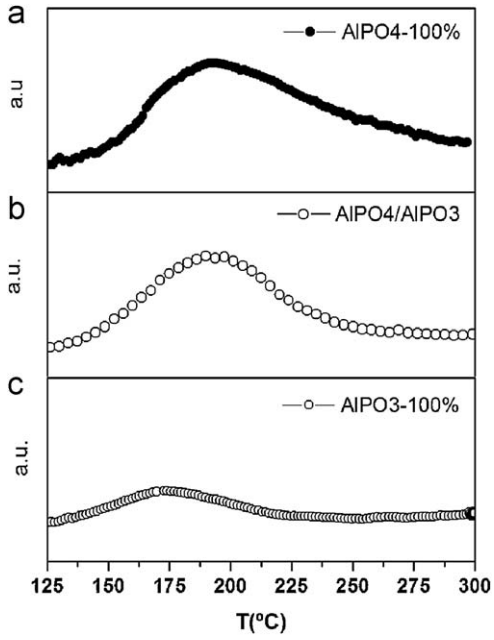

Fig. 6. NH_3 TPD profiles for: (a) Sample 1, (b) Sample 2, and (c) Sample 3.

and 50 ppm (Fig. 5). These signals are indicative of six- and four-coordinate Al centers, respectively. In the case of ALPO (Sample 1), deconvolution of the spectrum (Fig. 5a) indicates that the proportion of octahedral to tetrahedral aluminum sites is 37–63%. In the same way, the ^{27}Al MAS NMR data show that the Al_{octa}:Al_{tetra} ratio increases with the phosphite content: 71:29 (%) and 84:16 (%) for Samples 2 (Fig. 5b) and 3 (Fig. 5c), respectively. Moreover, this increase in the Al_{octa} proportion also appears reflected in the position of the resonance signals, which slightly shift towards lower field with the phosphite content (from ca. 45 to 52 ppm and −9 to −2 ppm for tetra and octahedral Al sites, respectively). These observations, which are consistent with a certain rise of alumina-like nanodomains, seem to account for the need of compensating the lower connectivity provided by phosphite anions when compared to the phosphate ones. At the same time, the observed increase in the proportion of octahedral aluminum sites with the phosphite content also appears as a necessity for making feasible the adequate interactions among the inorganic polyanions and the micelles. Indeed, in the absence of ion mediated species, the self-assembling stabilization of both aluminum phosphate and/or phosphite materials constitute examples of surfactant-templated materials formed through an S^+I^- ionic mechanism [46]. The charge matching at the interface must occur between cationic surfactant aggregates and anionic Al-phosphate and/or Al-phosphite moieties. Thus, the Al-phosphate/phosphite walls must retain a certain negative net-charge in the parent-as-prepared aluminum phosphite materials.

On the basis of the NMR data, it seems reasonable to propose that the Al-phosphate/phosphite walls are able to compensate the positive surfactant charge ($CTMA^+$) through two different mechanisms involving different inorganic groups at the pore wall surface: (1) the $\equiv P–O^-$ anionic units (form phosphate groups connected to aluminum atoms) and (2) the $Al–O^-$ groups at the surface. As the phosphite content increases, the effectiveness of the mechanism involving $\equiv P–O^-$ groups logically diminishes in a gradual way, and finally results inoperative for Sample 3. This "drawback" must be solved by the reinforcement of the charge matching mechanism involving the Al centers. In fact, the presence of $Al–O^-$ groups at the wall surface would make possible to neutralize the charge of $CTMA^+$ cations on account of the ability of the aluminum species to increase their coordination number from IV to VI (by interaction with water molecules and/or hydroxyl groups). Then, the structure of the wall surface in Sample 3 may be thought of as mainly defined by an alternating network of hydroxylated octahedral aluminum sites and phosphite groups, which would be supported on a rich alumina-like core (according to the phosphorus defective Al/P stoichiometry).

Shown in Fig. 6 are the NH_3-TPD profiles corresponding to samples of all the mesoporous solids. As can be observed, Samples 1 and 2 originates very similar desorption profiles consisting of one asymmetric and broad peak with a maximum at around 190 °C and a long tail, which extends until ca. 400 °C. Similar asymmetric profiles have been described as typical of layered and porous (micro and meso) metal phosphates, and explained basis on the presence of Br½nsted acid sites of different strength in the solids [47–50]. Amorphous aluminum phosphates synthesized at

low or moderate temperatures only present mild Br½nsted acid sites due to hydroxyl groups associated to P atoms and their acidity can be enhanced by hydrogen bonding to Al–OH groups [51]. In these solids the formation of Lewis acid sites only occurs when samples are heated at temperatures above 500 °C due to the formation of surface defects during the surface dehydroxylation [51,52]. Then, in our samples, only mild or low Br½nsted acid sites of similar strength can be expected. In the case we are dealing with, the total amount of desorbed NH_3 is similar for Samples 1 and 2 (1.59×10^{-4} and 1.44×10^{-4} NH_3 mol/g, respectively), what correspond to approximately 1.5–2.0 acid sites/nm^2. This seemingly striking result can be understood, at least at a qualitative level, taking into account the different proportions of phosphate/phosphite groups and/or octahedral vs. tetrahedral Al sites in both solids. Thus, the evolution from Sample 1 to 2 implies a significant lowering in the number of acid HPO_4 groups (from 100% to 51%), but, in compensation, there is a concomitant increase in the number of octahedral Al sites (from 37% to 71%) able to provide acidic Al–O–H^+ centers at the surface. Both counterweighting trends results in a certain constant total acidity. In contrast, the Sample 3 profile differs both in the location of the desorption-peak maximum (ca. 170 °C; lower acid strength) and essentially in the number of acid sites (3.55×10^{-5} NH_3 mol/g, 0.42 acid sites/nm^2). In practice, in the case of Sample 3 the total elimination of acid phosphate groups only is partially compensated by a relatively moderate increase (ca. 13% with regards to Sample 2) in the proportion of octahedral (potentially acid) Al–O–H^+ centers.

4. Conclusions

As occurs in the case of organically templated open-framework phosphites [12], the partial or total substitution of phosphite for phosphate groups in ALPOs is not a simple exchange because of the significant differences existing between both anions. The consequent effects become reinforced when truly porous structures are achieved, given that the phosphite P–H bonds usually are directed or located in the pore voids and, in some sense, can be viewed as a surface functionalization. In these cases, the higher covalence and non acidic character of the P–H bond in comparison with the P–O–H phosphate links strongly affects the material surface nature and reactivity and, in an indirect way, the mesopore accessibility. In this paper we describe for the first time the synthesis and characterization of mesoporous materials containing phosphite anions. The low connectivity provided by the phosphite entities (with regard to the phosphate groups) is compensated, from a structural point of view, by an increase of the proportion of six-coordinated aluminum sites. On the other hand, the character of the hydrogen phosphite atoms as "dead ends" (they do not bridge to atoms other than phosphorus) necessarily located at the wall surface induces a certain heterogeneity along the mesoporous walls, which could be thought of as constructed from a rich-alumina core coated by an aluminum phosphite shell.

Taking into account the compositional and structural continuity in the Al–phosphite–phosphate system (as occurs for the Al–phosphate–phosphonate materials), it would be possible to modulate the surface properties of these materials through a fine stoichiometric tuning.

Acknowledgments

This research was supported by the Spanish Ministerio de Ciencia y Tecnología (under Grant CTQ2006-15456-C04-03) and the Generalitat Valenciana (under Grant GV/2007/001). JEH and MPC thank the MEC for R&C and Juan de la Cierva contracts, respectively.

References

[1] S.T. Wilson, B.M. Lok, C.A. Messina, T.R. Cannon, E.M. Flanigan, J. Am. Chem. Soc. 104 (1982) 1146.
[2] M.E. Davis, C. Saldariaga, C. Montes, J. Garces, C. Crowder, Nature 331 (1988) 698.
[3] S. Coluccia, E. Gianotti, L. Marchese, Mater. Sci. Eng. C 15 (2001) 219.
[4] P. Tynjälä, T. Pakkanen, Microporous Mesoporous Mater. 20 (1998) 363.
[5] B. Bujoli, H. Roussière, G. Montavon, S. Laïb, P. Janvier, B. Alonso, F. Fayon, M. Petit, D. Massiot, J.-M. Bouler, J. Guicheux, O. Gauthier, S. Lane, G. Nonglaton, M. Pipelier, J. Léger, D.R. Talham, C. Tellier, Prog. Solid State Chem. 34 (2006) 257.
[6] S.V. Kononova, M.A. Nesmeyanova, Biochemistry 67 (2002) 184.
[7] S. Yamanaka, M. Matsunaga, M. Hattori, J. Inorg. Nucl. Chem. 43 (1976) 1343.
[8] S. Yamanaka, M. Matsunaga, M. Tanka, J. Inorg. Nucl. Chem. 41 (1978) 605.
[9] B. Bujoli, S. Lane, G. Nonglaton, M. Pipelier, J. Léger, D.R. Talham, C. Tellier, Chem. Eur. J. 11 (2005) 1981.
[10] A.K. Cheetham, G. Ferey, T. Loiseau, Angew. Chem. Int. Ed. 38 (1999) 3268.
[11] P. Amorós, M.D. Marcos, A. Beltrán, D. Beltrán, Curr. Opin. Solid State Mater. Sci. 4 (1999) 123.
[12] T. Rojo, J.L. Mesa, J. Lago, B. Bazan, J.L. Pizarro, M.I. Arriortua J. Mater. Chem, DOI: 10.1039/b808795b.
[13] C.T. Kresge, M.E. Leonowicz, W.J. Roth, J.C. Vartuli, J.S. Beck, Nature 359 (1992) 710.
[14] J.S. Beck, J.C. Vartuli, W.J. Roth, M.E. Leonowicz, C.T. Kresge, K.D. Schmitt, J.L. Schlenker, J. Am. Chem. Soc. 114 (1992) 10834.
[15] A. Stein, Adv. Mater. 15 (2003) 763.
[16] A. Sayari, Chem. Mater. 8 (1996) 1840.
[17] A. Corma, Chem. Rev. 97 (1997) 2373.
[18] J.Y. Ying, C.P. Mehnert, M.S. Wong, Angew. Chem. Int. Ed. 38 (1999) 56.
[19] G.J.A.A. Soler-Illia, C. Sanchez, B. Lebeau, J. Patarin, Chem. Rev. 102 (2002) 4093.
[20] F. Schüth, Chem. Mater. 13 (2001) 3184.
[21] M. Tiemann, M. Fröba, Chem. Mater. 13 (2001) 3211 (and references therein).
[22] T. Kimura, Chem. Mater. 15 (2003) 3742.
[23] J. El Haskouri, C. Guillem, A. Beltrán, J. Latorre, D. Beltrán, P. Amorós, Eur. J. Inorg. Chem. (2004) 1804.
[24] J. El Haskouri, C. Guillem, A. Beltrán, J. Latorre, D. Beltrán, P. Amorós, Chem. Mater. 16 (2004) 4359.
[25] S. Cabrera, J. El Haskouri, S. Mendioroz, C. Guillem, J. Latorre, A. Beltrán, D. Beltrán, M.D. Marcos, P. Amorós, Chem. Commun. (1999) 1679.
[26] S. Cabrera, J. El Haskouri, C. Guillem, J. Latorre, A. Beltrán, D. Beltrán, M.D. Marcos, P. Amorós, Solid State Sci. 2 (2000) 405.
[27] J.G. Verkade, Acc. Chem. Res. 26 (1993) 483 (and references therein).
[28] J. El Haskouri, S. Cabrera, M. Caldés, C. Guillem, J. Latorre, A. Beltrán, D. Beltrán, M.D. Marcos, P. Amorós, Chem. Mater. 14 (2002) 2637.
[29] S. Cabrera, J. El Haskouri, J. Alamo, A. Beltrán, D. Beltrán, S. Mendioroz, M.D. Marcos, P. Amorós, Adv. Mater. 11 (1999) 379.
[30] J. El Haskouri, D. Ortiz de Zárate, C. Guillem, A. Beltrán, M. Caldes, M.D. Marcos, D. Beltrán, J. Latorre, P. Amorós, Chem. Mater. 14 (2002) 4502.
[31] L. Fernández, P. Viruela-Martín, J. Latorre, C. Guillem, A. Beltrán, P. Amorós, J. Mol. Struct.: TEOCHEM. 850 (2008) 94.
[32] K. Maeda, Y. Kiyozumi, F. Mizukami, Angew. Chem. Int. Ed. Engl. 33 (1994) 2335.
[33] K. Maeda, J. Akimoto, Y. Kiyozumi, F. Mizukami, J. Chem. Soc. Chem. Commun. (1995) 1033.
[34] K. Maeda, J. Akimoto, Y. Kiyozumi, F. Mizukami, Angew. Chem. Int. Ed. Engl. 34 (1995) 1199.
[35] K. Maeda, Y. Hashiguchi, Y. Kiyozumi, F. Mizukami, Bull. Chem. Soc. Jpn. 70 (1997) 345.
[36] L.-J. Sawers, V.J. Carter, A.R. Armstrong, P.G. Bruce, P.A. Wright, B.E. Gore, J. Chem. Soc. Dalton Trans. (1996) 3159.
[37] K. Popov, H. Rönkkömäki, L.H.J. Lajunen, Pure Appl. Chem. 73 (2001) 1641.
[38] A. Martell, L.G. Sillén, Stability Constants of Metal-Ion Complexes, The Chemical Society, London, 1964 p. 525.
[39] C.F. Baes, R.E. Mesmer, The Hydrolysis of Cations, Wiley, New York, 1976.
[40] S. Inagaki, S. Guan, Y. Fukushima, T. Ohsuma, O. Terasaki, J. Am. Chem. Soc. 121 (1999) 9611.
[41] B.J. Melde, B.T. Holland, C.F. Blanford, A. Stein, Chem. Mater. 11 (1999) 3302.
[42] T. Asefa, M.J. MacLachlan, N. Coombs, G.A. Ozin, Nature 402 (1999) 867.
[43] T. Kimura, Y. Sugahara, K. Kuroda, Microporous Mesoporous Mater. 22 (1998) 115.
[44] Z. Luan, D. Zhao, H. He, J. Klinowski, L. Kevan, J. Phys. Chem. B 102 (1998) 1250.
[45] Y. Khimyak, J. Klinowski, J. Mater. Chem. 12 (2002) 1079.
[46] Q. Huo, D.I. Margolese, U. Ciesla, P. Feng, T.E. Gier, P. Sieger, R. Leon, P.M. Petroff, F. Schüth, G.D. Stucky, Nature 368 (1994) 317.

[47] G. Bagnasco, J. Catal. 159 (1996) 249.
[48] G. Liu, Z. Wang, M. Jia, X. Zou, X. Zhu, W. Zhang, D. Jiang, J. Phys. Chem. B 110 (2006) 16953.
[49] H. Li, B. Shen, X. Wang, S. Shen, Energy Fuels 20 (2006) 21.
[50] J. Wang, J. Song, C. Yin, Y. Ji, Y. Zou, F.-S. Xiao, Microporous Mesoporous Mater. 117 (2009) 561.
[51] A. Corma, Chem. Rev. 95 (1995) 559.
[52] C. Morterra, G. Magnacca, Catal. Today 27 (1996) 497.